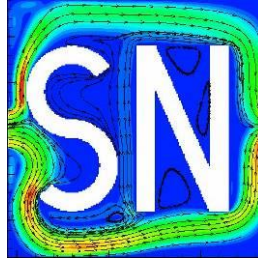


Turbulent Flow Over Backward-Facing Step
SmartNumerics Simulation Solutions Inc.



June 10, 2020

Copyright SmartNumerics Simulation Solutions Incorporated © 2020, All Rights Reserved.

Table of Contents

1.0 Introduction	1
2.0 Using k-ω 2006 Model with Lim = 0	3
3.0 Using k-ω 2006 Model with Lim = 0.875	5
4.0 Using SST Model without Vorticity	7
5.0 Using SST Model with Vorticity	9
References	11

1.0 Introduction

This validation test case is based on the experiments of Driver and Seegmiller [5] in a low-speed wind tunnel. They studied turbulent flow in a channel with a backward facing step having a height of 1.27 cm. The channel started one meter upstream of the step where the turbulent boundary layer was tripped using sandpaper. The channel height aft of the step was eight times the step height (10.16) cm. The channel was 12 times wider than it was high to minimize three-dimensional effects in the separated region downstream of the step. The freestream velocity was 44.2 m/s at atmospheric temperature and pressure corresponding to a Mach number of 0.128.

Based on experimental values of the ratio of stream-wise and transverse velocity fluctuations to the flow speed, the turbulence intensity at the center of the channel four step-heights upstream of the step is about 1.8%. The experiments were performed in a low-speed wind tunnel at NASA AMES.

The wall boundary layer thickness was 1.9 cm (1.5 step heights) and the Reynolds number (based on momentum thickness) was 5,000 at a location 4 step heights upstream of the step. Thus, the boundary layer was fully turbulent before passing over the step. Wall static pressure orifices were placed at intervals of $\frac{1}{2}$ step height downwind of the step. A vortical flow region formed downstream of the step. The reattachment point was 6.26 ± 0.1 step heights (7.95cm) downstream of the step.

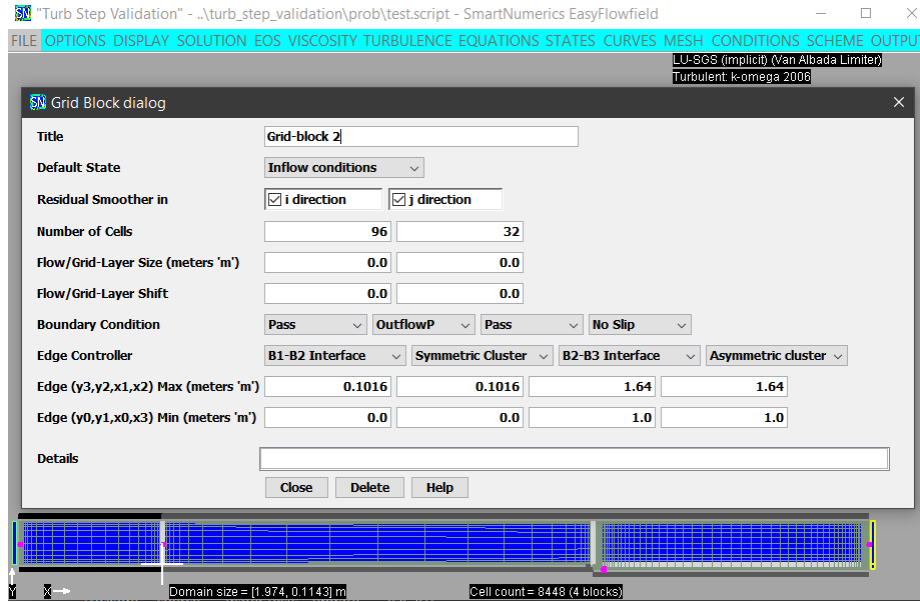


Fig. 1: Grid and grid-block dialog used for simulation of flow over a step.

Figure 1 displays the four-block grid and the dialog used to generate the block on the upper right (B2). An inflow condition with fixed mass flow and total temperature is imposed on the leftmost block (B0) and a slip condition is imposed at the top and bottom of that block. An outflow condition with fixed static pressure is imposed on the right faces of the two blocks on the right (B2, B3). The walls are modeled using no-slip boundary conditions (grey). EasyFlowfield can apply a wall roughness condition, but the sandpaper trip is not modelled since the turbulence models were developed assuming fully turbulent flow. The grid-line distribution at each edge of a block is controlled by an edge controller which overrides the grid-layer size and shift values. Some of the edge controllers connect adjacent blocks (white).

The condition used for the initial state, and the reference for the inflow and outflow boundaries was a static pressure of 100,402 Pascals, a static temperature of 296.75 °K, and a flow speed of 42.2 m/s. This corresponds to a Mach number of 0.122. However, the maximum Mach number is 0.128 and the maximum flow speed is 44.2 m/s four step-heights upstream of the step. The simulation was run using a global time-step size for the first 3,000 cycles since it was unstable using a local time-step size. The LU-SGS solver was used with a CFL of 3,000. The HLLC flux was used with the van Albada limiter.

2.0 Using $k-\omega$ 2006 Model with $\text{Lim} = 0$

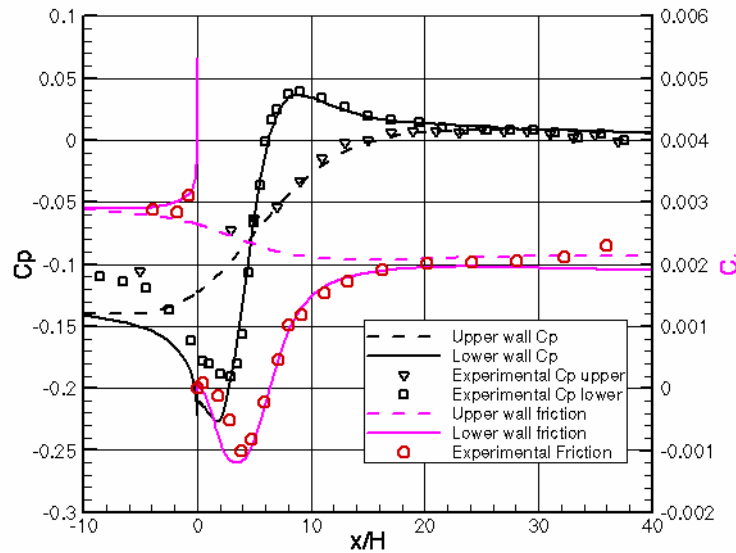


Fig. 2: Pressure and friction for turbulent flow over a step ($k-\omega$ 2006, $\text{Lim} = 0$).

Figure 2 displays the friction and pressure coefficients at the top and bottom walls computed using the $k-\omega$ 2006 turbulence model of Wilcox [2] with the stress limiter weight set to zero. The pressure coefficient from the simulation is computed using

$$c_p = 2 \frac{p_w - p_{\text{ref}}}{\rho_{\text{ref}} U_{\text{ref}}^2}$$

where p_w is the local pressure at the wall, p_{ref} is set to 100,400 Pascals, ρ_{ref} is the inflow density, and U_{∞} is the maximum velocity four steps upstream of the step.

The skin friction coefficients from the simulation is computed using

$$c_f = 2 \frac{\rho_w (u^*)^2}{\rho_{\text{ref}} U_{\text{ref}}^2} \text{sign}(u^*)$$

using the local friction velocity, u^* , output by the solver. Here, ρ_w is the local density at the wall. The friction velocity is output with a negative sign if the flow along the wall is reversed. Thus, the plotted friction is negative where the flow reverses.

The point of reattachment is 6.36 step heights (within 1.6%). The values of C_p and C_f are too low upstream of and just downstream of the step but are a good fit to experiment further downstream. The inflow turbulence intensity is 1% and the inflow eddy viscosity is one tenth of the molecular viscosity. The reattachment point increases to 6.37 step heights if the turbulence intensity is decreased to 0.25%. The reattachment point increases to 6.39 step heights if the turbulence intensity is increased to 4% and is 6.38 step heights if the inflow eddy viscosity is reduced by a factor of 10. The reattachment point increases to 6.46 step heights (within 3.2%) if the number of cells in both directions is doubled and to 6.37 step heights (within 1.8%) if quadrupled.

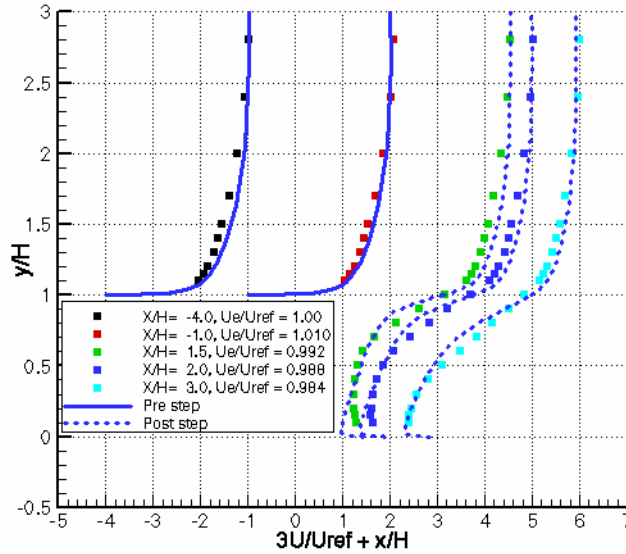


Fig. 3a: Stream-wise velocity profiles for flow over a step (k- ω 2006, Lim = 0).

Figure 3a displays velocity profiles at various values of step height on either side of the step. The velocity ratio U/U_{ref} multiplied by three is plotted using a displacement of x/H . The values from the simulation were taken from the column of cells closest to the location where the experimental data was measured. Here U_{ref} is the full-stream velocity 4 step heights upstream of the step.

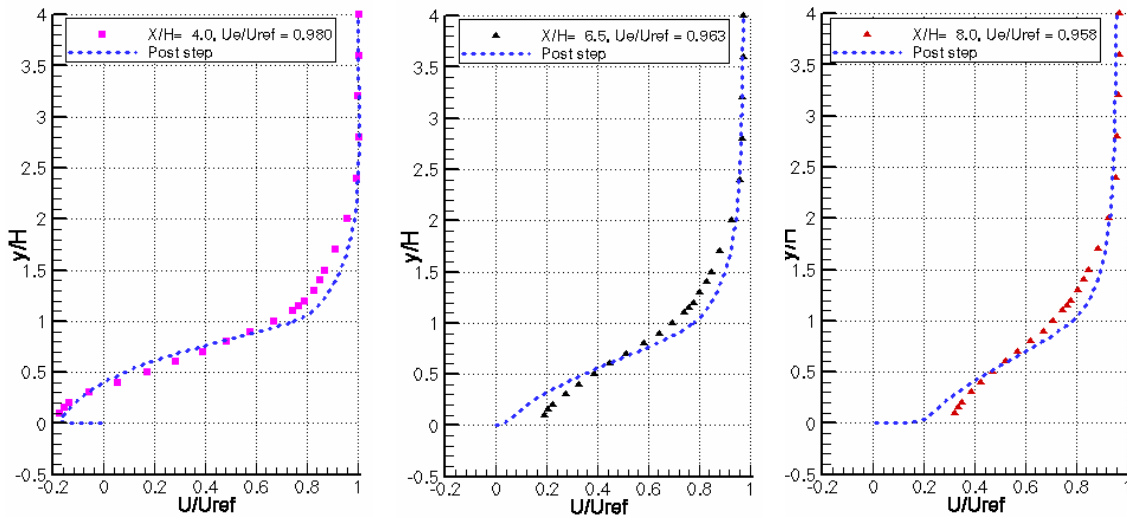


Fig. 3b: Stream-wise velocity profiles for flow over a step (k- ω 2006, Lim = 0).

Figure 3b compares the velocity ratio from the simulation at 3.7, 6.3, and 8.15 step-heights to the experimental values at 4, 6.5, and 8 step heights, respectively.

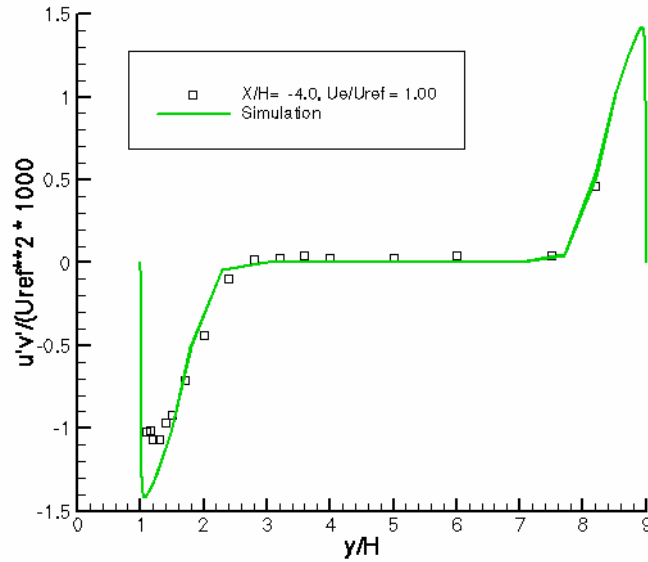


Fig. 4: Plot of normalized $\overline{u'v'}$ vs y/H for flow over a step (k- ω 2006, Lim = 0).

Figure 4 displays a plot of normalized turbulent shear stress, $\overline{u'v'}$ four step heights upstream of the step. For the simulation, this is approximated using

$$\overline{u'v'} = -\frac{\mu^T}{\rho} \left(\frac{\partial u}{\partial y} + \frac{\partial v}{\partial x} \right)$$

where μ_T is the eddy viscosity and ρ is the local density. The solver can output velocity gradients computed at the cell corners (nodes). The fit to the experimental values is good at most points.

3.0 Using k- ω 2006 Model with Lim = 0.875

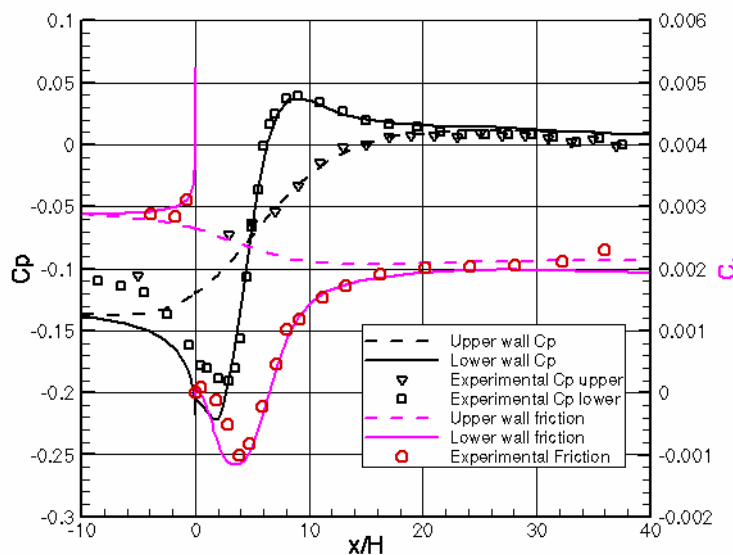


Fig. 5: Pressure and friction for turbulent flow over a step (k- ω 2006, Lim = 0.875).

Figure 5 displays the friction and pressure coefficients at the top and bottom walls computed using the $k-\omega$ 2006 turbulence model with the stress limiter weight set to the standard value of 0.875. The point of reattachment is 6.49 step heights (within 4.2%).

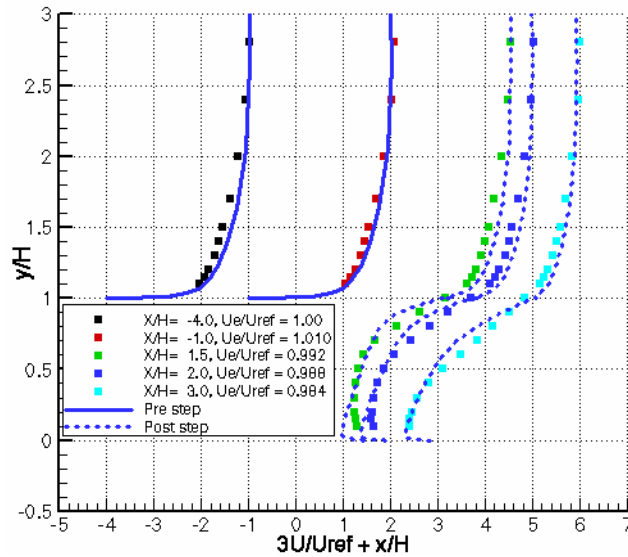


Fig. 6a: Stream-wise velocity profiles for flow over a step ($k-\omega$ 2006, $Lim = 0.875$).

Figure 6a displays the corresponding velocity profiles at various values of step height on either side of the step.

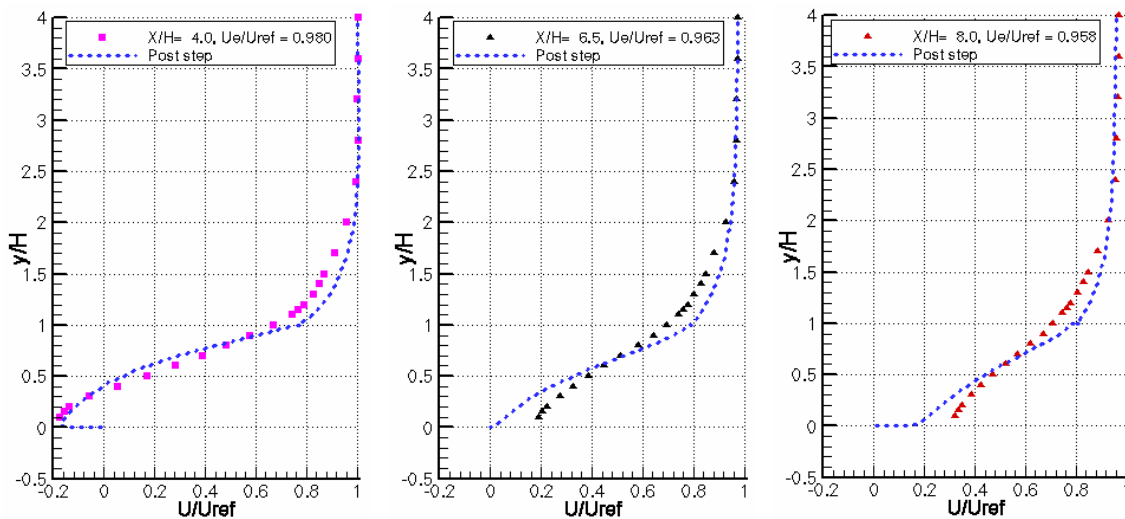


Fig. 6b: Stream-wise velocity profiles for flow over a step ($k-\omega$ 2006, $Lim = 0.875$).

Figure 6b compares the velocity ratio from the simulation at 3.7, 6.3, and 8.15 step-heights to the experimental values at 4, 6.5, and 8 step heights, respectively.

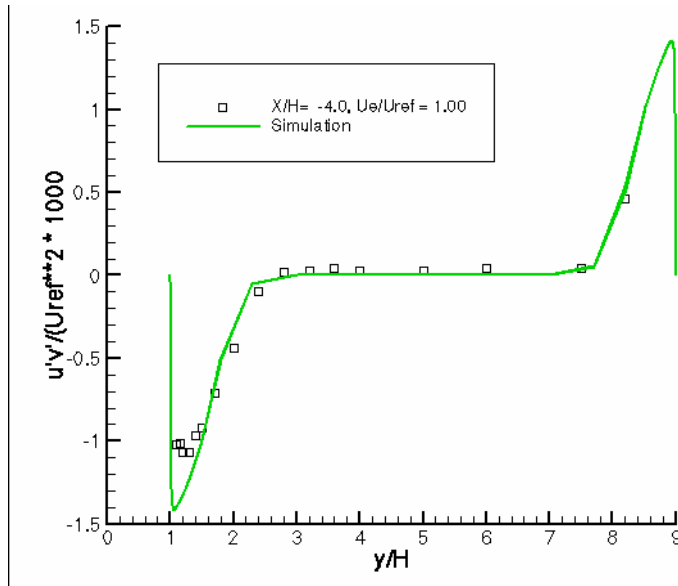


Fig. 7: Plot of normalized $\overline{u'v'}$ vs y/H for flow over a step ($k-\omega$ 2006, $\text{Lim} = 0.875$).

Figure 7 displays a plot of normalized turbulent shear stress, $\overline{u'v'}$ four step heights upstream of the step.

4.0 Using SST Model without Vorticity

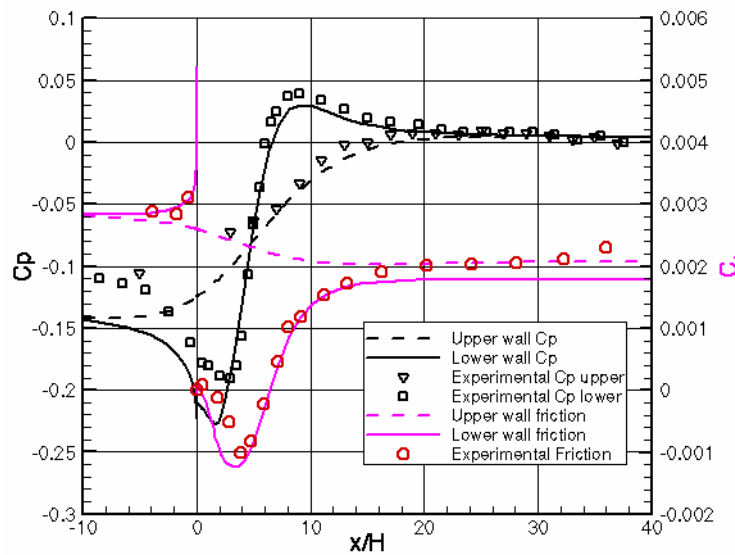


Fig. 8: Pressure and friction for turbulent flow over a step (SST, no vortex src.).

Figure 8 displays the friction and pressure coefficients at the top and bottom walls computed using the SST turbulence model of Menter [3] without use of vorticity in the turbulence source term. The point of reattachment is 6.44 step heights (within 2.9%).

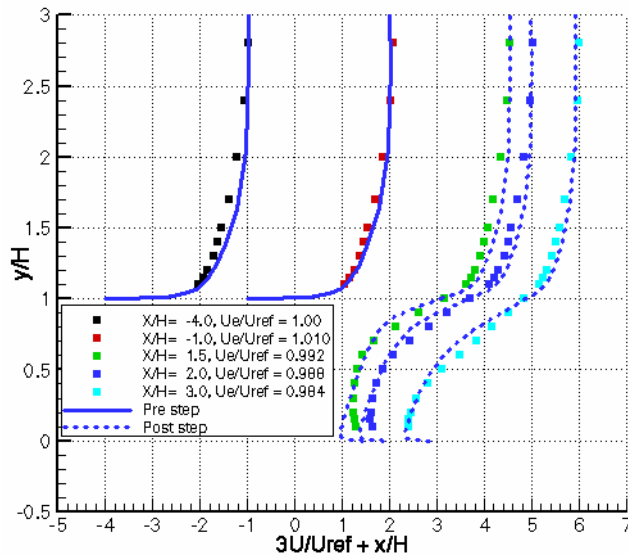


Fig. 9a: Stream-wise velocity profiles for flow over a step (SST, no vortex src.).

Figure 9a displays the corresponding velocity profiles at various values of step height on either side of the step.

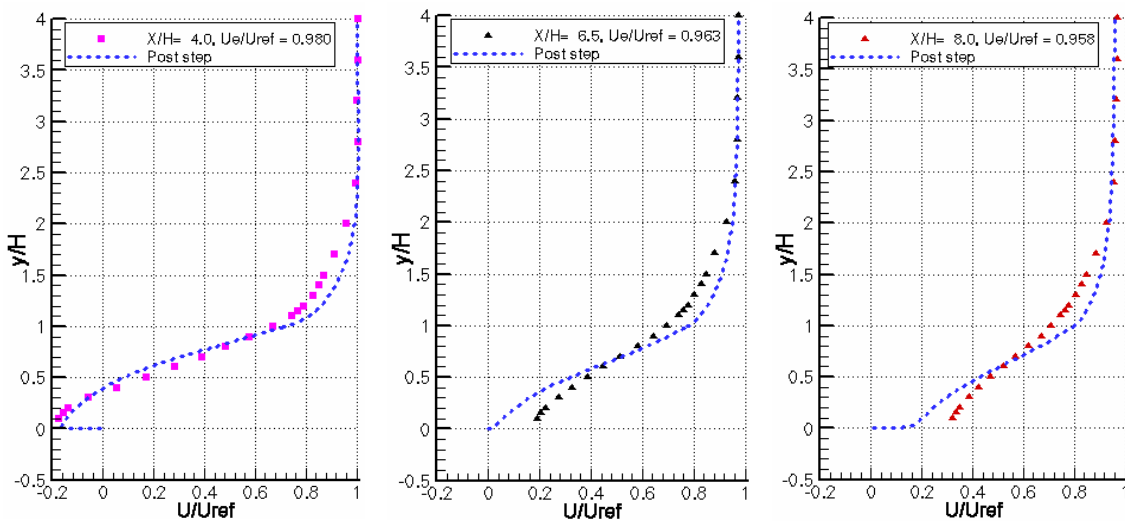


Fig. 9b: Stream-wise velocity profiles for flow over a step (SST, no vortex src.).

Figure 9b compares the velocity ratio from the simulation at 3.7, 6.3, and 8.15 step-heights to the experimental values at 4, 6.5, and 8 step heights, respectively.

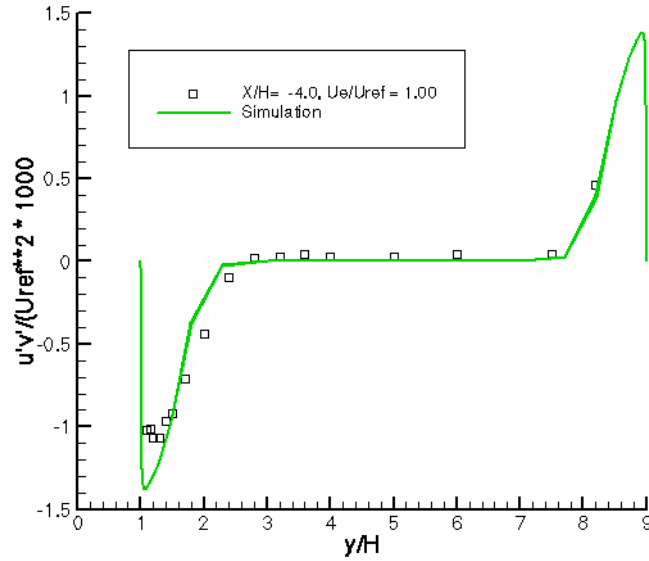


Fig. 10: Plot of normalized $\overline{u'v'}$ vs y/H for flow over a step (SST, no vortex src.).

Figure 10 displays a plot of normalized turbulent shear stress, $\overline{u'v'}$ four step heights upstream of the step.

5.0 Using SST Model with Vorticity

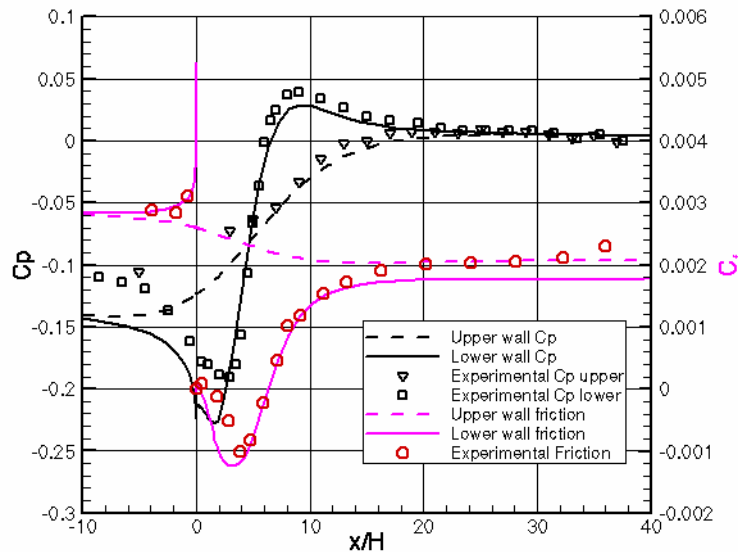


Fig. 11: Pressure and friction for turbulent flow over a step (SST, vortex src.).

Figure 11 displays the friction and pressure coefficients at the top and bottom walls computed using the SST turbulence model of Menter [3] with use of vorticity in the turbulence source term. The point of reattachment is 6.32 step heights (within 0.96%).

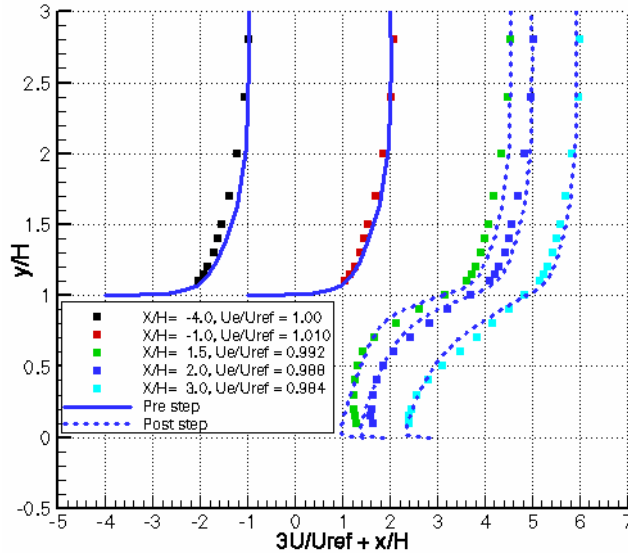


Fig. 12a: Stream-wise velocity profiles for flow over a step (SST, vortex src.).

Figure 12a displays the corresponding velocity profiles at various values of step height on either side of the step.

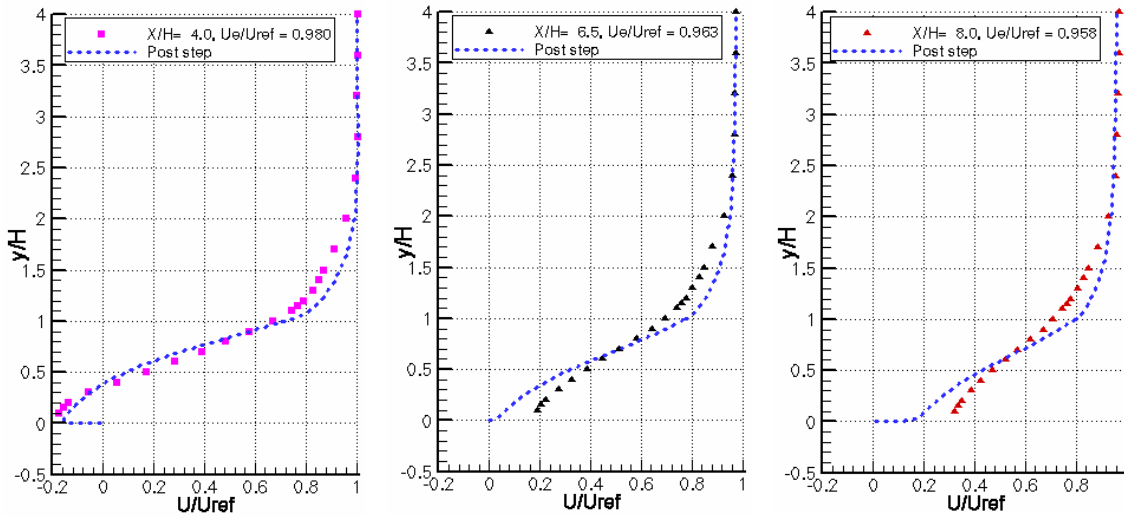


Fig. 12b: Stream-wise velocity profiles for flow over a step (SST, vortex src.).

Figure 12b compares the velocity ratio from the simulation at 3.7, 6.3, and 8.15 step-heights to the experimental values at 4, 6.5, and 8 step heights, respectively.

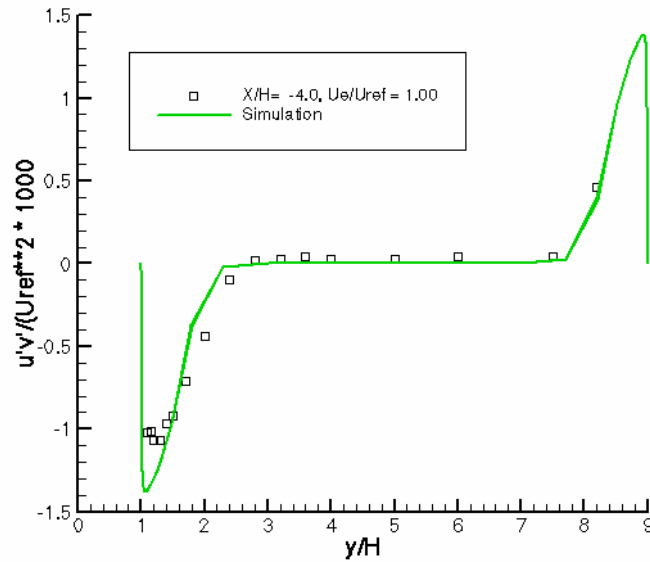


Fig. 13: Plot of normalized $\overline{u'v'}$ vs y/H for flow over a step (SST, vortex src.).

Figure 13 displays a plot of normalized turbulent shear stress, $\overline{u'v'}$ four step heights upstream of the step.

References

- [1] Driver, D. M., Seegmiller, H. L., "Features of a Reattaching Turbulent Shear Layer in Divergent Channel Flow," AIAA Journal, Vol. 23, No. 2, pp. 163-171, Feb. 1985.
- [2] Wilcox, D. C., Turbulence Modeling for CFD, 3rd ed., DCW Industries Inc., 2006.
- [3] Menter, F. R., Improved two-equation $k-\omega$ Turbulence Models for Aerodynamic Flows, NASA TM-103975, 1992.